Proceedings of the ASME INTERNATIONAL MECHANICAL ENGINEERING CONGRESS & EXPOSITION
IMECE2010
November 12-18, 2010, Vancouver, British Columbia, Canada

IMECE2010-40363

STRUCTURAL HEALTH MONITORING OF COMPOSITE STRUCTURES WITH PIEZOELECTRIC WAFER ACTIVE SENSORS

Victor Giurgiutiu
University of South Carolina
Columbia, South Carolina, USA

ABSTRACT

Piezoelectric wafer active sensors (PWAS) are lightweight and inexpensive enablers for a large class of structural health monitoring (SHM) applications such as: (a) embedded guided-wave ultrasonics, i.e., pitch-catch, pulse-echo, phased arrays; (b) high-frequency modal sensing, i.e., the electro-mechanical (E/M) impedance method; (c) passive detection (acoustic emission and impact detection). The focus of this paper will be on the challenges and opportunities posed by the composite structures as different from the metallic structures on which this methodology was initially developed. After a brief introduction, the paper discusses damage modes in composites. Then, it reviews the PWAS-based SHM principles. It follows with a discussion of guided wave propagation in composites and PWAS tuning effects. Finally, the paper presents some experimental results with damage detection in composite specimens. The paper ends with conclusions and suggestions for further work

INTRODUCTION

Structural health monitoring (SHM) is an emerging technology with multiple applications in the evaluation of critical structures. The goal of SHM research is to develop a monitoring methodology that is capable of detecting and identifying, with minimal human intervention, various damage types during the service life of the structure. Numerous approaches have been utilized in recent years to perform structural health monitoring [1-4]; they can be broadly classified into two categories: passive methods and active methods. Passive SHM methods (such as acoustic emission, impact detection, strain measurement, etc.) have been studied longer and are relatively mature; however, they suffer from several drawbacks which limit their utility (need for continuous monitoring, indirect inference of damage existence, etc.). Active SHM methods are currently of greater interest due to their ability to interrogate a structure at will. One of the promising active SHM methods utilizes arrays of piezoelectric wafer active sensors (PWAS) bonded to a structure for both transmitting and receiving ultrasonic waves in order to achieve damage detection[5-7]. When used to interrogate thin-wall structures, the PWAS are effective guided wave transducers by coupling their in-plane motion with the guided wave particle motion on the material surface. The in-plane PWAS motion is excited by the applied oscillatory voltage through the d31 piezoelectric coupling. Optimum excitation and detection happens when the PWAS length is in certain ratios with the wavelength of the guided wave modes. The PWAS action as ultrasonic transducers is fundamentally different from that of conventional ultrasonic transducers. Conventional ultrasonic transducers act through surface tapping, i.e., by applying vibration pressure to the structural surface. The PWAS transducers act through surface pinching, and are strain coupled with the structural surface. This allows the PWAS transducers to have a greater efficiency in transmitting and receiving ultrasonic surface and guided waves when compared with the conventional ultrasonic transducers.

There has been a marked increase in recent years in the use of composite materials in numerous types of structures, particularly in air and spacecraft structures. Composites have gained popularity in high-performance products that need to be lightweight, yet strong enough to take high loads such as aerospace structures, space launchers, satellites, and racing cars. Their growing use has arisen from their high specific strength and stiffness, when compared to metals, and the ability to shape and tailor their structure to produce more aerodynamically efficient configurations[8].

For this reason, it is important to study how active SHM methods (which were initially developed for isotropic metallic structures) can be extended to reliably detecting damage in these new types of materials, which are multi-layered and anisotropic. One of the most troubling forms of damage in laminar composites is low velocity impact damage. This type of damage can leave no visual traces, but subsurface delaminations can significantly reduce the strength of the structure.

The present paper presents and discusses the challenges and opportunities related to the use of PWAS in generating and sensing ultrasonic guided waves in composite materials and how they can be used to detect damage in composite structures. The paper starts with a brief a presentation of the main composite materials damage types which are often different from those encountered in metallic structures. Then, it reviews the principles of PWAS-based SHM. Subsequently, the paper discusses the analytical challenges of studying guided waves in composites and shows how the concept of guided-wave tuning with PWAS can be applied in the case of composite structures: theoretical predictions and experimental tuning results are comparatively presented. Finally, the paper presents experimental results on detecting hole and impact damage in composite plates with PWAS-based pitch-catch and pulse-echo methods. Hole damage detection experiments were performed on unidirectional and quasi-isotropic plates, whereas impact damage detection experiments were performed only on quasi-isotropic plates. The paper ends with conclusions and suggestions for further work.

DAMAGE IN COMPOSITE MATERIALS

Composite materials combine the properties of two or more constituent materials in order to achieve properties that are not achievable by the individual constituents. For example, carbon fiber composites combine the extreme specific stiffness and strength of carbon fibers with the binding properties of a polymeric matrix. In general, composites can be created from any two materials (metals, ceramics, polymers, elastomers, glasses) that could be mixed in many ways (particulate inclusions, chopped-fiber, woven, unidirectional fibers, etc.); the final composite properties vary with (a) the choice of constituents, and (b) the composite architecture. For high-performance structural applications, laminate composites made up of high strength/stiffness unidirectional layers stacked at various angles have gained wide application. The choice of the orientation angles in the stacking sequence allows tailoring of the composite properties along certain preferential directions that are expected to experience highest operational loads. The simplest layup sequence is the 0/90 (cross-ply) laminate, which consists of alternating 0-deg and 90-deg layers (Figure 1). Some layup sequences such as 0/45/90 and 0/60/120 are dubbed 'quasi-isotropic' because they try to equalize the effective properties by applying the fibers in several directions.

The damage and failure of metallic structures is relatively well understood; their in-service damage and failure occurs mostly due to fatigue cracks that propagate under cyclic loading in metallic material. In contrast, the damage of composite materials occurs in many more ways than that of metals[9,10]. Composites fail differently under tension than they fail in compression, and the effect of fastener holes is much more complicated than in metals. In addition, the composites are prone to hidden damage from low velocity impact (e.g., the drop of a hand tool); such damage can be barely visible and may go undetected, but its effect on the degradation of the composite structure strength can be dramatic. These various damage aspects will be discussed briefly in the next sections.

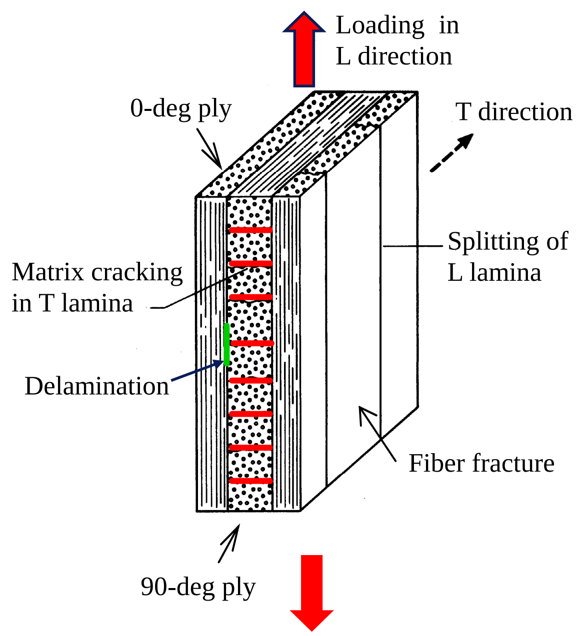

Figure 1: Longitudinal tension of a 0/90 composite laminate highlighting several damage modes: (a) matrix cracking in transverse (T) lamina; (b) splitting of longitudinal (L) laminae; (c) delamination between T and L laminae

Current design requirements for composite structures are much more stringent than for metallic structures. Military aircraft components have to comply with an Aircraft Structural Integrity Program (ASIP) following the JSSG 2006[11] and MIL-STD-1530[12] guidelines. Pre-existing manufacturing flaws and service-induced cracking are assumed to exist, even if undetected and the ASIP function is to manage this fact while preventing aircraft accidents and downtime. In general, metallic structures are allowed to exhibit a certain amount of sub-critical crack growth within the design life of the component. Detectable cracks are noted and managed as part of the maintenance and inspection process. In contrast, **no known delamination-cracks are allowed to exist** (much less grow) in composite structure. However, the composite components are generally designed to tolerate a certain size of undetectable damage. Of course, this additional 'safety margin' comes with a weight penalty, which could be mitigated through better understanding of composite damage detection and management mechanisms.

In order to satisfy the damage tolerance requirements, one has to demonstrate that an aircraft structure possesses adequate residual strength at the end of service life in the presence of an assumed worst-case damage, as for example that caused by a low-velocity impact on a composite structure. This may be accomplished by showing positive margins-of-safety at the maximum recommended load. Worst-case damage is defined as the damage caused by an impact event (e.g., a 1-in hemispherical impactor) at the lesser of the following two energy levels: (a) 100 ft-lb, or (b) energy to cause a visible dent (0.1-in deep).

IMPACT DAMAGE IN COMPOSITE STRUCTURES

Composite aerospace structures are prone to a particular type of damage that is not critical in metallic aerospace structures, i.e., **low-velocity impact damage**. Such damage may occur during manufacturing or in service due to, say, a hand tool being dropped onto a thin-wall composite part. When such an impact happens on a conventional metallic structural part, either the part is not damaged at all, or, if it is damaged, then it shows clearly as an indent or scratch. In composite structures, a similar impact may damage the structure without leaving any visible marks on the surface (so called **barely visible damage**). In this case, the impact result takes the form of **delaminations** in the composite layup. (A more drastic impact may also show spalling on the back side, while having no visible marks on the front side).

Delamination due to barely visible impact damage may not have a large effect on the tension strength of the composite, but it can significantly **diminish the composite compression strength** (delaminated plies have a much weaker buckling resistance than the same plies solidly bonded together). Both component buckling strength and local buckling strength may be affected; when a fastening hole is present, this effect may be even worse. For this reason, manufacturing companies place a strong emphasis on testing the **open-hole compression strength after impact** of their composite structures. Detection of delaminations due to barely visible impact damage is a major emphasis in composite SHM research.

DAMAGE DETECTION IN COMPOSITE MATERIALS

We have seen that the inherent macroscopic anisotropy and multi-material architecture of the composite materials results in internal damage types which are significantly different from those encountered in isotropic metallic materials. Currently, one of the most commonly encountered damage types in composite materials is that caused by low-velocity impact; this damage susceptibility (which is not encountered in metallic structures) is mainly due to the low interlaminar strength of conventional composite layups. Significant degradation of the mechanical properties can easily occur as a result of low-velocity impact even for barely visible damage. Different types of damage may be encountered in the impacted region, including matrix (resin) cracking, delaminations (interlaminar cracking) and broken fibers. In the future, as composite structures accumulate years of service, other damage types related to fatigue effects are also expected to become significant.

To date, much effort has been put into identifying reliable non-destructive evaluation (NDE) techniques for the detection, location, and characterization of composite materials damage with a special attention to subsurface delaminations due to manufacturing defects or to low-velocity impacts. Thermography, shearography, radiography, and ultrasonics are among the most commonly used NDE techniques[13,14]. These NDE techniques require stripping the aircraft and even removal of individual components; they employ bulky transducers, operate with point scanning, and, in general, are time consuming, labor intensive, and expensive. As a result, the current cost of composite structures inspection is very high, at least one order of magnitude greater than for metallic structures[15]. In order for composite structures to be economically viable and to realize their full design potential, it is essential that their operation and maintenance is conducted in a safe and economical manner, on par with that of existing metallic structures. For this reason, the development of new composite damage detection methods that can be applied rapidly and reliably to detect critical composite flaws is an ongoing concern. The permanently attached damage sensing technologies developed under the structural health monitoring (SHM) thrust are a promising research direction because, when implemented, they would permit the interrogation at will of the composite structures and the reliable and credible detection of internal damage in order to increase flight safety and reduce operational costs. This technology, though promising, is still in its infancy and many theoretical and experimental challenges still have to be resolved, as illustrated next.

PWAS PRINCIPLES

Piezoelectric wafer active sensors (PWAS) are the enabling technology for active SHM systems. PWAS couples the electrical and mechanical effects (mechanical strain, S_{ij}, mechanical stress, T_{kl}, electrical field, E_k, and electrical displacement D_j) through the tensorial piezoelectric constitutive equations

$$\begin{aligned} S_{ij} &= s^E_{ijkl} T_{kl} + d_{kij} E_k \\ D_j &= d_{jkl} T_{kl} + \varepsilon^T_{jk} E_k \end{aligned} \qquad (1)$$

where, s^E_{ijkl} is the mechanical compliance of the material measured at zero electric field ($E = 0$), ε^T_{jk} is the dielectric permittivity measured at zero mechanical stress ($T = 0$), and d_{kij} represents the piezoelectric coupling effect. PWAS utilize the d_{31} coupling between in-plane strain and transverse electric field. A 7-mm diameter PWAS, 0.2 mm thin, weighs a bare 78 mg and costs around ~$1 each. PWAS are lightweight and inexpensive and hence can be deployed in large numbers on the monitored structure. Just like conventional ultrasonic transducers, PWAS utilize the piezoelectric effect to generate and receive ultrasonic waves. However, PWAS are different from conventional ultrasonic transducers in several aspects:

1. PWAS are **firmly coupled with the structure** through an adhesive bonding, whereas conventional ultrasonic transducers are weakly coupled through gel, water, or air.
2. PWAS are **non-resonant devices** that can be tuned selectively into several guided-wave modes, whereas conventional ultrasonic transducers are resonant narrow-band devices.
3. PWAS are inexpensive and can be deployed in large quantities on the structure, whereas conventional ultrasonic transducers are expensive and used one at a time.

By using Lamb waves in a thin-wall structure, one can detect structural anomaly, i.e., cracks, corrosions, delaminations, and other damage. Because of the physical, mechanical, and piezoelectric properties of PWAS transducers, they act as both transmitters and receivers of Lamb waves traveling through the structure. Upon excitation with an electric signal, the PWAS generate Lamb waves in a thin-wall structure. The generated Lamb waves travel through the structure and are reflected or diffracted by the structural boundaries, discontinuities, and damage. The reflected or diffracted waves arrive at the PWAS where they are transformed into electric signals.

PWAS transducers can serve several purposes[16]: (a) high-bandwidth strain sensors; (b) high-bandwidth wave exciters and receivers; (c) resonators; (d) embedded modal sensors with the electromechanical (E/M) impedance method. By application types, PWAS transducers can be used for (i) **active sensing of far-field damage** using pulse-echo, pitch-catch, and phased-array methods, (ii) **active sensing of near-field damage** using high-frequency E/M impedance method and thickness-gage mode, and (iii) **passive sensing of damage-generating events** through detection of low-velocity impacts and acoustic emission at the tip of advancing cracks. Damage detection using PWAS phased arrays can detect both broadside and offside cracks independently with scanning beams emitting from a central location.

GUIDED WAVES IN COMPOSITES

The evaluation of structural integrity using Lamb wave ultrasonics has long been acknowledged as a very promising technique. Several investigators[17-19] have envisioned the inspection of large metallic plates from a single location using transducer arrays where each element acts as both transmitter and receiver. Guided signals are generated at different angles around the transducer positions and the signal reflections from the boundaries are processed for damage detection. This configuration is very promising for isotropic material but might have some limitations for fibrous composite structures due to the change in properties with fiber direction. In recent years, numerous investigations have explored Lamb wave techniques for the detection of damage in composite laminates[10,20,21]. In order to take full advantage of Lamb wave techniques for composite damage detection, one needs to first understand and model how guided waves propagate in composite structures which is much more complicated than in isotropic metallic structures.

The guided waves propagating in composite structures are more difficult to model than those propagating in isotropic metallic structures because of the composite material is inherent anisotropy and multilayered, with each layer having a different orientation. A composite plate is made of N layers; each layer is made of unidirectional fibers hence they are layers of orthotropic properties; however, the layer orientation varies from layer to layer. Consider a wave propagating in the material and assume that the angle between the fiber direction and the direction of wave propagation for the k^{th} layer is θ_k. Define the global coordinate system x_1, x_2, x_3 such that x_1 is aligned with the direction of wave propagation. Also define a local coordinate system x_1', x_2', x_3' such that x_1' is parallel to the fiber direction (principal axes). The stiffness matrix of the k^{th} layer can be written as

$$C = T_1^{-1} C' T_2 = \begin{bmatrix} c_{11} & c_{12} & c_{13} & 0 & 0 & c_{16} \\ c_{12} & c_{22} & c_{23} & 0 & 0 & c_{26} \\ c_{13} & c_{23} & c_{33} & 0 & 0 & c_{36} \\ 0 & 0 & 0 & c_{44} & c_{45} & 0 \\ 0 & 0 & 0 & c_{45} & c_{44} & 0 \\ c_{16} & c_{26} & c_{36} & 0 & 0 & c_{66} \end{bmatrix} \quad (2)$$

where C' is the layer stiffness in local principal axes, and C is the stiffness matrix in global axes aligned with the direction of wave propagation, whereas T_1 and T_2 are the coordinate transformation matrices for stress and strain, respectively. Assume that the wave propagation direction is parallel to the plane $x_1 x_2$ and assume that the displacement solution can be written as

$$\left(u_1, u_2, u_3\right) = \left(U_1, U_2, U_3\right) e^{i\xi\left(x_1 + \alpha x_3 - vt\right)} \quad (3)$$

where ξ is the wavenumber in the x_1 direction, $v = \omega/\xi$ is the phase velocity, ω is the circular frequency, α is an unknown parameter equal to the ratio between the wavenumber in the x_3 direction and the wavenumber in the x_1 direction, and U_i is the displacement amplitude. The equation of motion in each composite layer can be solved to yield the expressions for the displacement field (u_1, u_2, u_3) in terms of the layer properties and boundary conditions at the top and bottom of the layer. (The characteristic equation for wave propagation in an orthotropic layer is more complicated than that for isotropic materials, but still solvable.)

After the wave propagation inside each layer is setup in terms of layer properties and boundary conditions at the top and bottom contact surfaces with the other layers, the next step is to solve for wave propagation in the complete composite laminate. This is achieved by linking together the composite layers by imposing equilibrium and compatibility conditions at the interfaces, i.e., matching stresses and displacements. Two solution approaches exist: (a) the transfer matrix approach; and (b) the global matrix approach. In the transfer matrix (TM) approach[22-26], the tractions and strains at the bottom of one layer are described in terms of those of the top of the layer through a transfer matrix, which depends on the properties and orientation of that specific layer, i.e.,

$$\begin{Bmatrix} \{u_k^+\} \\ \{\sigma_k^+\} \end{Bmatrix} = [A_k] \begin{Bmatrix} \{u_k^-\} \\ \{\sigma_k^-\} \end{Bmatrix} \tag{4}$$

where the matrix A_k is the layer-transfer matrix for the k^{th} layer. The transfer between two consecutive layers is achieved by imposing displacements continuity force equilibrium at the interfaces between consecutive layers. Thus, boundary conditions at the top of the composite plate (e.g., wave excitation) are propagated from layer to layer to the bottom of the plate through the sequential layer to layer transfer. In the end, we relate the displacements and stresses of the top of the layered plate to those at its bottom through the overall transfer matrix, A, given by

$$A = \prod_{k=1}^{N} A_k \tag{5}$$

Thus, a small linear system of equation is setup in which the boundary conditions at the top of the plate are relate to the boundary conditions at bottom of the plate. To find the dispersion curves and modeshapes, one assumes traction-free conditions at both top and bottom surfaces and solves the resulting homogenous system in terms of unknown top and bottom displacements. The resulting eigenvalue problem yields eigen wave numbers and the associate eigen displacements at the top and bottom of the plates. The eigen wave numbers yield the phase velocities at the assumed frequency; the dispersion curves are then obtained by repeating the process over a frequency range. The eigen displacements are propagated through the matrix transfer process through all the layers in order to determine the thickness mode shape of that particular guided wave mode. Though simple in formulation, the TM method suffers from numerical instability because error accumulates in the layer transfers. To address the numerical instabilities, Rokhlin and Wang[27,28] address this numerical instability issue by introducing the layer stiffness matrix and using an efficient recursive algorithm to calculate the global stiffness matrix for the complete laminate. The layer stiffness matrix relates the stresses at the top and bottom of the layer with the corresponding displacements. The terms in the matrix have only exponentially decaying terms and hence the transfer process becomes more stable.

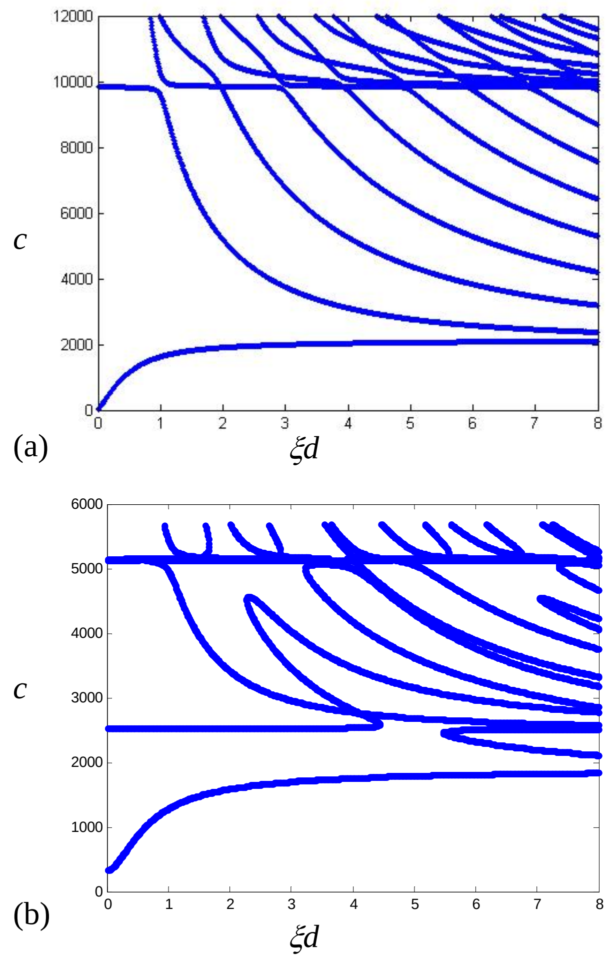

Figure 2 Dispersion curves for unidirectional 65/35 graphite-epoxy plate: (a) $\theta = 0^\circ$; (b) $\theta = 36^\circ$; (d) $\theta = 90^\circ$. Note: c is the wave speed in m/s; ξd is the dimensionless wavenumber-half thickness product

DISPERSION CURVES FOR COMPOSITE STRUCTURES

We coded the TM approach following Nayfeh26. Figure 2 shows the dispersion curves derived for a unidirectional composite plate made of one layer of 65% graphite 35%

epoxy. These dispersion curves depend on the propagation direction, θ; the cases $\theta = 0°$ and 36° are presented in Figure 2. It is apparent that, for $\theta = 0°$ (i.e., wave propagating along the fiber direction) the dispersion curves are clearly decoupled into quasi-antisymmetric (A0, A1, A2,…), quasi symmetric (S0, S1, S2, …), and quasi-shear horizontal (SH0, SH1, SH2,…) wave modes. However, this in not the case for the off-axis direction $\theta = 36°$, in which case the three mode types are strongly coupled. The wave velocity is higher when the wave propagates along the fiber direction. As the angle of the wave propagation direction increases, the phase velocity decreases till reaching a minimum in the direction perpendicular to the fiber. This is due to the fact that along the fiber the material stiffness is greater than in all the other directions and it decreases while θ increases.

Next, we analyzed various composite layups. The dispersion curves for a $\left[(0/45/90/\text{-}45)_{2s}\right]$ quasi-isotropic layup were developed. Over a large ξd range, the dispersion curves showed a complicated pattern of tightly coupled composite-plate wave modes; however, a zoom-in to low ξd values revealed a simpler pattern in which the A0, S0, SH0 modes were clearly traceable.

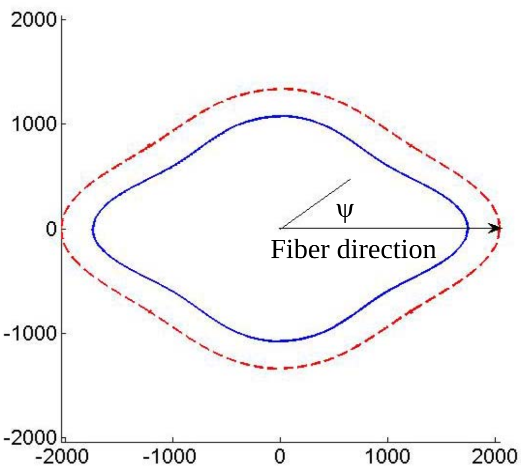

Figure 3 Directional dependence of wave propagation wave front in unidirectional 65% graphite 35% epoxy plate (solid blue line: $fd = 400$ kHz-mm ; dash red line: $fd = 1,700$ kHz-mm) Note: axes units are dimensionless for relative illustration of wave front distortion

GROUP VELOCITY IN COMPOSITE STRUCTURES

In isotropic metallic plates, the calculation of group velocity, c_g, a.k.a., energy velocity, c_E, is rather straight forward, since it is done by differentiation of frequency with respect to wave number, i.e., $c_g = \dfrac{\partial \omega}{\partial \gamma}$. In anisotropic fibrous composite, the calculation of group velocity is rather more complicated and it has to use the slowness curve. The phase slowness is the inverse of the phase velocity; hence, the phase slowness curve shows how the relative arrival time of a plane wave propagating in an anisotropic plate varies with the direction of wave propagation. Assume we want to find the group velocity c_E for a wave propagating along direction θ with respect to the fiber direction. By definition, the group velocity vector is perpendicular to the phase slowness curve. By drawing the normal to the slowness curve at point P we determine the direction of the group velocity vector c_E; this direction is oriented along angle ψ. By elementary geometry, the group velocity magnitude is given by $c_E = \dfrac{c}{\cos\phi}$ where $\phi = \psi - \theta$.

Knowing the magnitude of c_E and the angle ψ for each propagation direction, one can construct the wave surface.
Figure 3 shows the corresponding wave front contours. It is apparent that the wave propagation is faster along the fiber direction than across the fiber direction. This observation is consistent with the fact that the fibrous composite is much stiffer along the fibers than across the fibers. The fact that the wave front contour varies with the frequency-thickness product is also apparent in Figure 3.

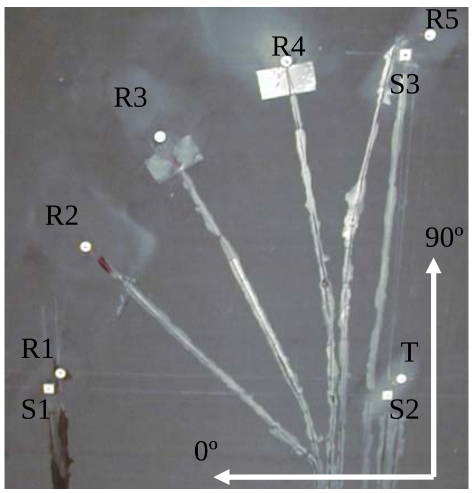

Figure 4 Experiment setup measuring directional wave speeds in a $[(0/45/90/\text{-}45)2]_S$ plate 1240-mm x 1240-mm with 2.25-mm thickness. The plate was laminated from T300/5208 unidirectional tape

TUNED GUIDED WAVES IN COMPOSITE STRUCTURES

The tuning between PWAS transducers and guides waves in isotropic metallic plates is relatively well understood and modeled30. The gist of the concept is that manipulation of PWAS size and frequency allow for selective preferential excitation of certain guided wave modes and the rejection of other guided wave modes, as needed by the particular SHM application under consideration. A similar tuning effect is also possible in anisotropic composite plates, only that the analysis is more complicated due to the anisotropic wave propagation characteristics inherent in composite materials.

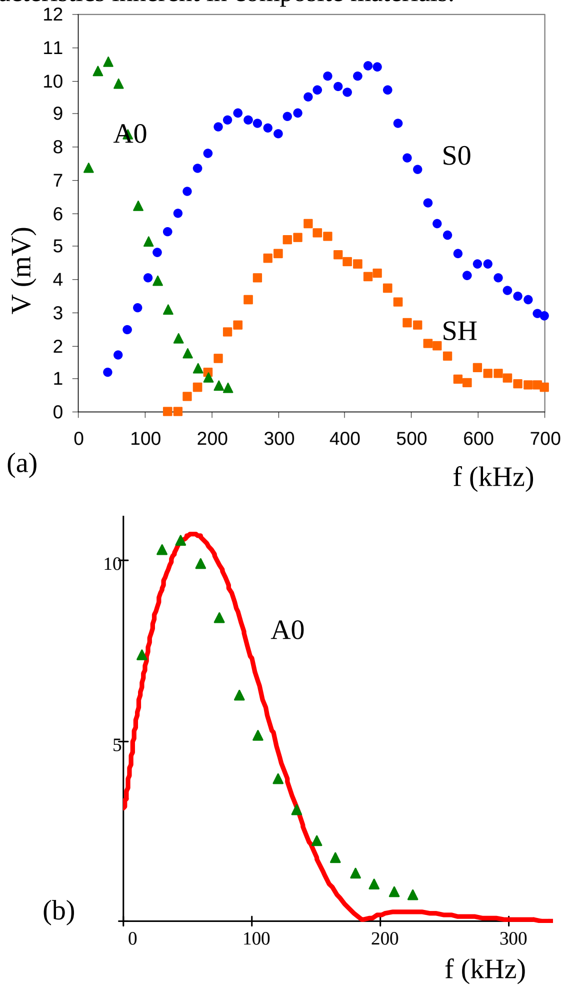

Figure 5 Tuning of PWAS guided waves in composites: (a) quasi-A0 mode, quasi-S0 mode, quasi-SH0 mode. (b) comparison of theoretical prediction (full line) vs. experimental values for A0 mode

We performed experiments on a composite plate with PWAS receivers installed at various directions from the PWAS transmitter. Figure 4 shows the experimental setup: a 1240-mm x 1240-mm quasi-isotropic plate was used. The plate had an overall thickness of 2.25 mm; the plate a $[(0/45/90/-45)2]_S$ layup from T300/5208 carbon fiber unidirectional tape. Figure 4 shows the central part of the composite plate where 7-mm round PWAS transducers (0.2-mm thick, American Piezo Ceramics APC-850) were installed. The PWAS denoted with the letter T was the transmitter while those denoted with R were the receivers (R1…R5). The distance between the receivers and the transmitter was 250 mm. The step angle between sequential receivers was $\Delta\theta = 22.5°$. In addition, a pair of 7-mm square PWAS were placed along the fiber direction, with S1 being the transmitter and S2 the receiver.

Smoothed 3-count tone-burst excitation signals were used. The signal frequency was swept from 15 kHz to 600 kHz in steps of 15 kHz. At each frequency, the wave amplitude and the time of flight for all the waves present were collected. Since carbon fiber is electrically conductive, the composite plate could be used as ground and only a single excitation wire had to be cabled to each PWAS transducer. We found that the ground quality affects the signal strength; to obtain a strong signal, a good electrical ground was achieved through bonding a sheet of copper on the composite surface. In this way the signal was strong and consistent during the experiments.

Three guided wave modes were detected: quasi-S0, quasi-A0, and quasi-SH0. Figure 5a shows the experimentally measured signal amplitudes for the three guided waves. The quasi-A0 reaches a peak response at around 50 kHz and then decreases. In fact, the A0 mode disappears as soon as the quasi-SH wave appears. The quasi-S0 mode reaches a peak at 450 kHz and then decreases. The quasi-SH0 mode reaches a peak response at around 325 kHz. Figure 5b shows a comparison between theoretical prediction and experimental values for the A0 mode; the match between theory and experiment is quite good, which gives confidence in our modeling approach.

EXPERIMENTAL RESULTS OF DAMAGE DETECTION IN COMPOSITE PLATES

We did a series of experiments to detect damage in composite plates. The first type of damage we used in our experiments was a small hole of increasing diameter. Holes are generally not a representative type of damage for composite structures; however, we decide to use holes first in our damage detection tests because this type of damage can be easily manufactured and reproduced with accuracy. The second type of damage we considered in our experiments was impact damage. This type of damage was produced using an inertial impactor. Details of these two types of experiments are given in the following two sections.

HOLE DAMAGE DETECTION IN UNIDIRECTIONAL COMPOSITE SPECIMENS

We performed experiments to detect small holes of increasing size in unidirectional composite strips.

Two unidirectional strips were used for these experiments. Both strips we instrumented with two 7-mm round PWAS placed 150 mm apart. The PWAS transducers were used in pitch catch mode. In one experimental setup, the hole damage was placed directly in the pitch-catch path; since this placement is the most favorable for detection, we used this experiments to determine the detection threshold, i.e., the smallest detectable hole size. In the second experimental setup, we placed the hole offset by 20 mm from the pitch-catch path. Again, we performed detection experiments with holes of increasing size in order to determined the smallest detectible hole size in this less favorable condition. The hole size diameters increased in 11 steps from zero through 6.4 mm. The first readings were taken when the strips were undamaged (baselines). Than, we drilled a 0.8 mm hole on both, and we enlarged them in 11 steps till they reached 6.35 mm in diameter. All readings were recorded at 480 kHz. At this frequency we have a single strong S0 wave packet.

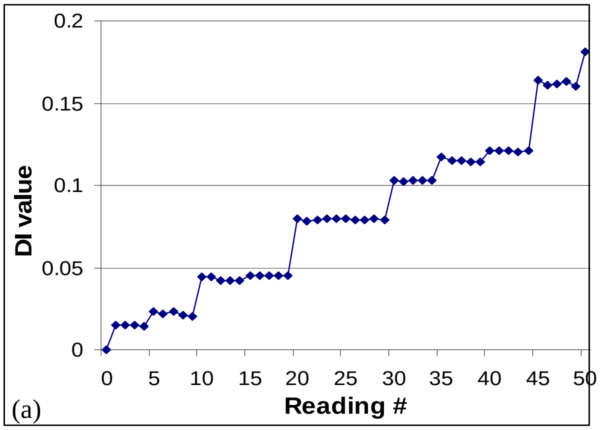

Figure 6 DI analysis of pitch-catch hole damage detection in an unidirectional composite strip

The collected data were analyzed with the damage index (DI) method. The DI value was computed with the root mean square deviation (RMSD) algorithm. The resulting DI values were plotted (Figure 6). The detection results for the case when the hole is directly in the pitch-catch path are given in Figure 6. The first five readings were for the baseline, i.e., for the pristine specimen without damage. The next five readings are for the specimen with the 0.8-mm hole, and so on. If we look at Figure 6a representing the results for the damage in the direct pitch-catch path, we note that, as soon as damage was inflicted on the specimen, the DI value changed. This indicates that the detection method is very sensitive to small damage. The next three groups on the plot in Figure 6a give the DI values for hole sizes of 0.8, 1.5, and 1.6 mm. We note that the change from 0.8 mm to 1.5 mm damage size produced a clear jump in the DI value, but the next two changes were much smaller; this seems to be consistent with the fact that the relative change from 1.5 mm to 1.6 mm is much smaller than from 0.8 mm to 1.5 mm. The DI values keep increasing with increasing hole size; the only anomaly is that no change was registered by the DI when the hole size increased from 2 mm to 2.4 mm. It is to notice that the biggest jumps in DI values (from reading 20 to reading 21 and from reading 45 to reading 46) were achieved for the biggest changes in hole size. Similar results were obtained for the detection of the hole placed offside from the pitch-catch path.

Figure 8a shows the 54-kHz detection results; at 54-kHz, only A0 mode was present. The wave velocity is 1580 m/sec; the wavelength is 29.3 mm. Figure 8 shows the box plot of the DI values for the three different PWAS pairs. As the hole diameter increases, the DI values for the two PWAS pairs close to the hole (p0-p13 and p1-p12) increases while the DI for the PWAS pair p5–p8 remain almost constant. We analyzed the data with statistical software (SAS) and we observed that with a significance of 99%, PWAS pair p1–p12 can detect the presence of a hole with at lest 2.77-mm diameter. On the other hand, the PWAS pair p0–p13 could detect the presence of a hole with the same 99% significance only when the hole diameter was at lest 3.18 mm. The DI for the PWAS pair p05-p08 did not show any significant change, as expected. Similar results were obtained for the other frequency cases. Other experiments conducted on this quasi isotropic composite specimen include pulse-echo detection of holes and detection of impact damage.

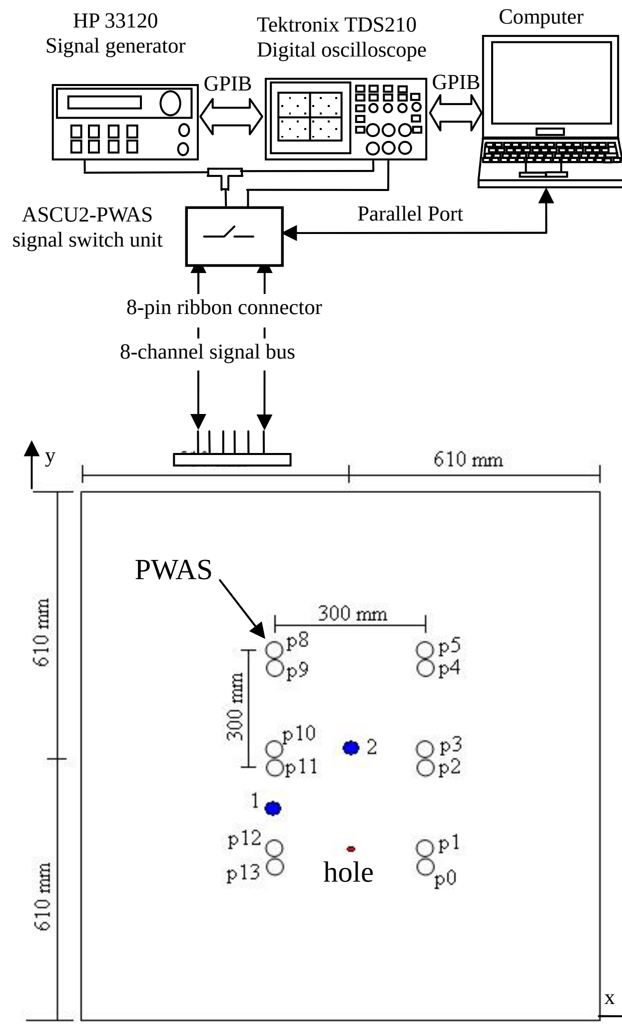

Figure 7 Experimental set-up for hole damage detection on quasi-isotropic composite panel: Featured on the plate are: 14 PWAS transducers (p0 through p13); one hole damage; two impact locations (1 and 2)

HOLE DAMAGE DETECTION IN A QUASI-ISOTROPIC COMPOSITE PLATE

In this set of experiments, we used a 1240-mm x 1240-mm quasi-isotropic plate with a $[(0/45/90/-45)2]_S$ layup of T300/5208 unidirectional tape; the overall thickness was 2.25 mm. Two damage types were considered: (a) drilled holes of increasing diameter; and (b) impact created with an inertial impactor. The experimental setup is shown in Figure 7. The two holes are marked as 'hole'. The impact location is marked as 1 and 2. A set of 12 PWAS transducers were installed in pairs as shown in Figure 7. The PWAS pairs were (p0,p1), (p2,p3), (p4,p5), (p8,p9), (p10,p11), (p12,p13). The distance between the PWAS pairs was 300 mm. The excitation signal was a 3-count 11-V smoothed tone burst. The data were collected automatically using an ASCU2 signal switch (Figure 7). We collected data from PWAS p0, p1, p5, p8, p12, p13. Each PWAS was in turn transmitter and receiver. Three frequency values were used: (i) $f = 54$ kHz, when only the A0 mode is present; (ii) $f = 225$ kHz, when only the S0 mode is present; and (iii) $f = 255$ kHz, when the S0 mode has maximum amplitude. Four sequential baseline readings were taken with the plate undamaged. Subsequent readings were taken after each damage type was applied to the plate. A hole of increasing size was drilled between PWAS p1 and p12 (see Figure 7). The location of the hole was halfway between these two PWAS. The diameter of the hole was increased in 14 steps from zero through ~ 6 mm. At each damage step, several readings were taken. Data processing consisted in comparing each reading with the baseline (reading 00) and calculating the damage index (DI). The DI value was computed with the root mean square deviation (RMSD) algorithm. We analyzed the DI data with statistical software (SAS) and stated our conclusions to a significance of 99%

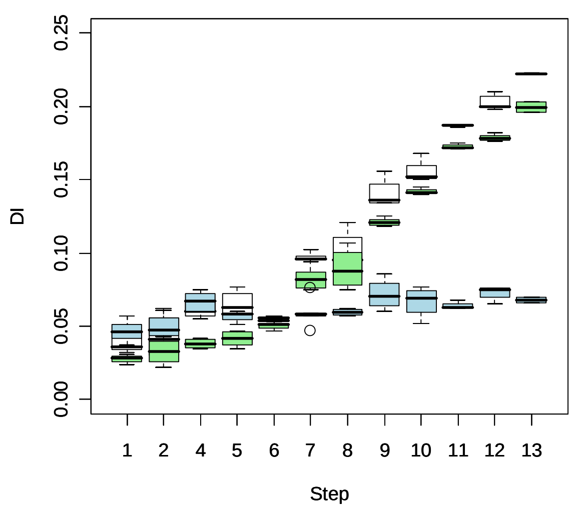

Figure 8 Pitch-catch hole detection results showing DI values at different damage step values and different PWAS pairs. (a) $f = 54$ kHz, i.e., when only A0 mode is present

CONCLUSION

This paper has presented how piezoelectric wafer active sensors (PWAS) can be used to detect damage in composite structures. PWAS are lightweight and inexpensive transducers that enable a large class of structural health monitoring (SHM) applications such as: (a) embedded guided-wave ultrasonics, i.e., pitch-catch, pulse-echo, phased arrays; (b) high-frequency modal sensing, i.e., the electro-mechanical (E/M) impedance method; (c) passive detection (acoustic emission and impact detection). The focus of this paper has been on the challenges and opportunities posed by the composite structures as different from the metallic structures on which this methodology was initially developed. After a brief introduction, the paper discussed the damage modes commonly met in aerospace composite structures. Then, it reviewed the PWAS-based SHM principles. It follows with a discussion of guided wave propagation in composites and PWAS tuning effects.

The paper presented experimental damage detection results in composites: (i) hole damage in unidirectional and quasi-isotropic plates; and (ii) impact damage in quasi-isotropic plates. In **unidirectional** carbon-epoxy composite strips, it was found that the **minimum detectable hole** size was 0.8 mm. The detection method used in these experiments was pitch-catch with 480-kHz tuned S0 waves. In **quasi-isotropic** carbon-epoxy composite plates, it was found that the **minimum detectable hole** size with 99% confidence was 2.77 mm. In these experiments, we used several tuned guided wave modes, A0 waves at 54 kHz; and S0 waves at 225 kHz and 255 kHz. The detection methods used in these experiments were both pitch-catch and pulse-echo. In the **impact damage** experiments, it was found that tuned A0 guided wave mode were much more effective in detecting impact damage in **quasi-isotropic carbon-epoxy plates** than S0 mode.

Further research needs to be done to better understand the interaction of guided waves with damage in composite materials and how various guide-wave types interact with various types of damage.

REFERENCES

[1] Doebling, S. W., Farrar, C. R., Prime, M. B., and Shevitz, D. W., "Damage Identification and Health Monitoring of Structural and Mechanical Systems From Changes in Their Vibration Characteristics: A Literature Review," Los Alamos National Laboratory Report LA-13070-MS, May 1996.

[2] Sohn, H., Farrar, C.R., Hemez, F. M., Shunk, D. D., Stinemates, S. W., Nadler, B. R., and Czarnecki, J. J., "A Review of Structural Health Monitoring Literature form 1996-2001," Los Alamos National Laboratory report LA-13976-MS, 2004.

[3] Farrar, C.R., Sohn, H., Hemez, F.M., Anderson, M.C., Bement, M.T., Cornwell, P.J., Doebling, S.W., Schultze, J.F., Lieven, N., Robertson, A.N., "Damage Prognosis: Current Status and Future Needs," Los Alamos National Laboratory Report, LA-14051-MS, 2004

[4] Rose, J.L., Soley, L., "Ultrasonic guided waves for the detection of anomalies in aircraft components", Materials Evaluation, Vol. 50, No. 9, pg. 1080-1086, 2000.

[5] Giurgiutiu, V., "Lamb Wave Generation with Piezoelectric Wafer Active Sensors for Structural Health Monitoring", *SPIE's 10th Annual International Symposium on Smart Structures and Materials and 8th Annual International Symposium on NDE for Health Monitoring and Diagnostics*, 2-6 March 2003, San Diego, CA, paper # 5056-17

[6] Giurgiutiu, V., Zagrai, A., Bao, J. J., Redmond, J. M., Roach, D., and Rackow, K. "Active Sensors for Health Monitoring of Aging Aerospace Structures," International Journal of COMADEM, Vol. 6, No. 1, pg 3–21, 2003.

[7] Giurgiutiu, V., Zagrai, A., Bao, J., "Damage Identification in Aging Aircraft Structures With Piezoelectric Wafer Active Sensors," Journal of Intelligent Material Systems and Structures, Vol. 15, No. 9–10, pg. 673–687, 2003.

[8] Soutis, C. and Beaumont, P.W.R., "Multi-scale modelling of composite material systems: The art of predictive damage modelling". Woodhead Publishing Ltd., ISBN-13: 978-1-85573-936-9, 2005.

[9] Tong L. and Soutis, C., "Recent Advances in Structural Joints and Repairs for Composites Materials" (Kluwer Academic Publishers, The Netherlands, ISBN 1-4020-1381-7) 2003.

[10] Diamanti, K., Soutis, C. and Hodgkinson, J. M. "Non-Destructive Inspection of Sandwich and Repaired Composite Laminated Structures". Composites Science & Technology, 65(13), (2005), 2059-2067.

[11] JSSG-2006: "Aircraft Structures, General Specification for", US Dept. of Defense Joint Specification Guide JSSG-2006, 30 Oct. 1998, http://www.everyspec.com/DoD/DoD+PUBLICATIONS/JSSG-2006_10206/.

[12] MIL-HDBK-1530, "Aircraft Structural Integrity Program, General Guidelines for" US Dept. of Defense Military Handbook, 4 Nov. 1996, http://www.everyspec.com/MIL-HDBK/MIL-HDBK+(1500+-+1799)/MIL_HDBK_1530_1844/.

[13] Heida, J. H., Konijnenberg, P. and 'tHart, W. G. J., (1995). Characterization of Impact Damage in Carbon-Epoxy Composites, *Impact and Dynamic Fracture of Polymers and Composites*, eds. Williams, J. G. and Pavan, A., Mech. Eng. Publications, London, ESIS 19: 359-370.

[14] Cawley, P., (1994). The Rapid Non-Destructive Inspection of Large Composite Structures, *Composites*, **25** (5): 351-357.

[15] Bar-Cohen, Y., (1999). In-Service NDE of Aerospace Structures -- Emerging Technologies and Challenges at the End of the 2nd Millennium, *NDT.net*, **4** (9): 1-21.

[16] Giurgiutiu, V. (2008) *Structural Health Monitoring with Piezoelectric Wafer Active Sensors*, Elsevier Academic Press, 760 pages, ISBN 978-0120887606, 2008.

[17] Worlton, D. C., (1957). Ultrasonic Testing with Lamb Waves, *NonDestructive Testing*, **15** (4): 218-222.

[18] Rose J. L. (1999) "Ultrasonic waves in layered media", Cambridge University Press, 1999.

[19] Wilcox, P., Lowe, M. and Cawley, P., (2000). Lamb and SH Wave Transducer Arrays for the Inspection of Large Areas of Thick Plates, *Review of Progress in Quantitative Nondestructive Evaluation*, eds. Thompson, D. O. and Chimenti, D. E., Plenum Press, New York, 1049-1056.

[20] Birt, E. A., (1998). Damage Detection in Carbon-Fibre Composites Using Ultrasonic Lamb Waves, *Insight*, **40** (5): 335-339.

[21] Diamanti, K., Soutis, C. and Hodgkinson, J. M. "Piezoelectric transducer arrangement for the inspection of large composite structures". Composites A, 38(4), (2007), 1121-1130.

[22] Thomson, W. T. (1950) "Transmission of elastic waves through a stratified solid medium," J. Appl. Phys., vol. 21, pp. 89–93, 1950.

[23] Haskell, N. A. (1953) "Dispersion of surface waves on multilayered media," Bull. Seism. Soc. Am., vol. 43, pp. 17–34, 1953.

[24] Kausel E., (1986) "Wave propagation in anisotropic layered media" *International Journal for Numerical Methods in Engineering*, Vol. 23, 1567-1578, 1986.

[25] Nayfeh A. H., (1991) "The general problem of elastic wave propagation in multilayered anisotropic media" Journal of Acoustical Society of America, 89 (4), Pt. 1, April 1991.

[26] Nayfeh A. H., (1995) "Wave propagation in layered anisotropic media with application to composites" Elsevier, 1995.

[27] Wang L., Rokhlin S. I., (2001) "Stable reformulation of transfer matrix method for wave propagation in layered anisotropic media", *Ultrasonics*, 39 (2001), 413-424.

[28] Rokhlin S. I., Wang L., (2002) "Stable recursive algorithm for elastic wave propagation in layered anisotropic media: Stiffness matrix method", Journal of Acoustic Society of America, June, 2002.

[29] Knopoff, L. (1964) "A matrix method for elastic wave problems", Bulletin of seismology society of America; v. 54; no. 1; p. 431-438, February 1964.

[30] Giurgiutiu, V. (2008) Structural Health Monitoring with Piezoelectric Wafer Active Sensors, Elsevier Academic Press, 760 pages, ISBN 978-0120887606, 2008.

